Leaching optimization and dissolution behavior of alkaline anions in bauxite residue

by Li, X., Ye, Y., Xue, S., Jiang, J., Chuan, W.U., Kong, X, Hartley,W. and Li, Y.

DOI: https://doi.org/10.1016/S1003-6326(18)64763-6

Li, X., Ye, Y., Xue, S., Jiang, J., Chuan, W.U., Kong, X, Hartley,W. and Li, Y. 2019. Leaching optimization and dissolution behavior of alkaline anions in bauxite residue. *Transactions of Nonferrous Metals Society of China*, 28(6), pp.1248-1255.

Leaching optimization and dissolution behavior of alkaline anions in bauxite residue

Xiao-fei LI [1], Yu-zhen YE[1], Sheng-guo XUE [1, 2], Chuan WU [1, 2], Xiang-feng KONG [1], William Hartley [3], Yi-wei LI [1]

[1] School of Metallurgy and Environment, Central South University, 932 Lushan South Road, Changsha, Hunan, 410083, PR China;

[2] Chinese National Engineering Research Center for Control & Treatment of Heavy Metal Pollution, Central South University, Changsha, 410083, PR China;

[3] Crop and Environment Sciences Department, Harper Adams University, Newport, Shropshire, TF10 8NB, United Kingdom.

Foundation item: Project (41371475) supported by the National Natural Science Foundation of China; Project (201509048) supported by the Environmental protection's special scientific research for Chinese public welfare industry.

Corresponding author: Sheng-guo XUE; Tel:13787148441; E-mail: sgxue70@hotmail.com (S.G. Xue); sgxue@csu.edu.cn

Abstract: Bauxite residue is a highly alkaline waste, containing soluble alkaline anions which present serious environmental concerns. This paper focuses on the dissolution behavior of alkaline anions and the kinetics of critical alkaline anions during water leaching. During a two stage leaching investigation, 86% of the soluble alkaline anions (CO_3^{2-}, HCO_3^-, $Al(OH)_4^-$, OH^-) were leached in 23 h at a L/S ratio of 2 ml/g. During the first stage, 88 % of alkaline anions were leached from the dissolution of free alkali. Alkalinity in the supernatant reached 69.78 mmol/L, with CO_3^{2-} accounting for 75 %. Carbonate leaching was controlled by solid film diffusion. The findings provide a scientific foundation for effectively regulating alkalinity within bauxite residue prior to disposal.

Key words: Bauxite residue; alkaline anions; carbonate; leaching optimization; dissolution behavior.

1. Introduction

Bauxite residue (BR or red mud) is a hazardous alkaline solid waste originating from the Bayer process [3, 4] which is used to extract alumina from bauxite ore. Bauxite is digested in a caustic liquor of sodium hydroxide and slaked lime to enhance refining [1, 2]. Globally, approximately 120 million tons of BR is produced per year and the global inventory reached more than 4 billion tons in 2015 [5, 6]. Numerous methods for the treatment and subsequent use of BR have been investigated [7-10], but the volume recycled is still small because of the risk from its strong alkalinity and salinity [11, 12]. The majority of BR continues to be stored in bauxite residue disposal areas (BRDA) and has the potential to contaminate the surrounding environment [13]. Dust for example, formed from the surface of BRDAs, contains elevated concentrations of free alkali (soluble) that may threaten the surrounding ecology [14-16]. Furthermore, storage of residues may cause dam collapse, whilst dissolution of soluble alkaline compounds will also cause environmental risk [17].

Recently, amendment with gypsum, neutralization using seawater, carbonation sequestration and waste acid interaction have been proposed to regulate the alkalinity [18-23]. All these methods could effectively reduce pH and regulate alkalinity, but few have been conducted successfully. Limited knowledge related to dissolution behavior and distribution of soluble alkaline anions prior to BR disposal, may be the main factor restricting large-scale application of these methods. Reducing soluble alkaline anions in the liquid phase is therefore considered as a more desirable environmental management goal [24]. Water leaching is a promising way to investigate the dissolution behavior and composition distribution of soluble alkaline anions in BR, and will be helpful for effectively regulating alkalinity. However, almost all research has focused on the leaching of sodium, rare earth and available metals [25-27]. Sodium may partially be dissolved by water leaching, but the dealkalization rate is less than 50 % [6]. Due to the existing forms of alkalinity, including free alkali and chemical bonded alkali in BR [28], alkaline compounds will dissolve until chemical equilibrium in the solution is reached (Eqs. (1)–(9)).

$$NaOH \rightarrow OH^- + Na^+ \quad (1)$$

$$NaAl(OH)_4 \rightarrow Al(OH)_4^- + Na^+ \quad (2)$$

$$Na_2CO_3 \rightarrow CO_3^{2-} + 2Na^+ \quad (3)$$

$$NaHCO_3 \rightarrow HCO_3^- + Na^+ \quad (4)$$

$$CaCO_3 \rightarrow Ca^{2+} + CO_3^{2-} \quad (5)$$

$$3CaO \cdot Al_2O_3 \cdot 6H_2O \rightarrow 3Ca^{2+} + 4OH^- + 2[Al(OH)_4]^- \quad (6)$$

$$[Na_6Al_6Si_6O_{24}] \cdot [2NaX \text{ or } Na_2X] \rightarrow 8Na^+ + 6H_4SiO_4 + 6Al(OH)_3 + 8X \ (X: OH^- \text{ or } CO_3^{2-}) \quad (7)$$

$$[Na_6Al_6Si_6O_{24}] \cdot 2[CaCO_3] + 26H_2O \rightarrow 6Na^+ + 2Ca^{2+} + 6H_4SiO_4 + 6Al(OH)_3 + 2HCO_3^- + 8OH^- \quad (8)$$

$$Ca_3Al_2(SiO_4)_x(OH)_{12-4x} \rightarrow 3Ca^{2+} + (6-4x)OH^- + xH_4SiO_4 + 2Al(OH)_3 \quad (9)$$

(Eqs. (6-9) interpreted from [29-31])

Therefore, leaching of sodium will not accurately illustrate the dissolution of soluble alkalinity due to the dissolution of chemical bonded alkali and other minerals. Furthermore, the leaching rate of sodium will not balance the dealkalization specification of BR [32]. The leaching behavior of soluble alkaline anions in water is currently vague, but is pivotal to a logical understanding of alkaline leaching principles. Additionally, limited attention has been given to dissolution behavior and composition distribution of soluble alkaline anions to regulate alkalinity. The lack of understanding of alkaline anion sources has undoubtedly led to a significant knowledge gap in relation to regulation.

The objectives of this paper were (1) to investigate the optimal leaching conditions (L/S ratio, temperature, time and leaching stage) of BR, (2) to determine alkaline dissolution behavior and reaction equilibrium, (3) to screen alkaline anions and analyze their leaching kinetics, and finally (4), to understand dissolution behavior, composition distribution and alkalinity contribution of alkaline anions in BR and provide a scientific foundation for regulating alkalinity of BR prior to disposal.

2. Experimental

2.1 Materials

Raw BR (PRM) was collected from the Guangxi Branch, Aluminum Corporation of China Limited. Residue samples were thoroughly homogenized, oven dried at 65 °C for 48 h, and subsequently sieved (100 mesh). Soluble cations were determined using inductively coupled plasma atomic emission spectroscopy (ICP-AES) (Table 1). Mineral composition of the PRM was

performed by X-ray powder diffraction (XRD).

2.2 Methods

Leaching investigations consisted of three experiments:

Single factor experiments were conducted to assess L/S ratio, leaching temperature and leaching time respectively. The L/S ratio was set at 1, 2, 3, 4, 5, 6 and 7 mL/g, leaching temperature was controlled at 10, 15, 20, 25, 30, 35 and 40 °C, and leaching time controlled at 1, 2, 3, 5, 8, 13, 18 and 23 hrs.

For the second investigation, three factors and three levels were designed and it was conducted to acquire optimized leaching conditions. The leaching stage experiment was operated under the optimized conditions achieved above and the leaching stages were varied from 1 to 6 to investigate the origin and content of alkaline anions by each leaching stage. The leaching rate of alkaline anions from the dissolution of free alkali was obtained.

BR (20 g) was mixed with deionized water in a beaker, stirred vigorously by hand for 15 seconds, then sealed with a plastic membrane to prevent air flow. The experiment was conducted in a temperature controlled water bath. Leachates were filtered through SHZ-D (III) vacuum suction filters. pH, alkaline anions and aluminum concentration of leachates were immediately analyzed. The pH measurements were carried out using a PHS-3C and the content of hydroxide was calculated from pH data. Soluble Al was determined by an Inductively Coupled Plasma Auto Emission Spectrometer and aluminate was calculated from the Al concentration [4, 26].

Carbonate and bicarbonate were determined by double indicator-neutralization titration using 0.005 M H_2SO_4 [23]. Initially, a 5 mL leachate was diluted with 10 mL of deionized water, 0.05 mL phenolphthalein was added to the solution and then titrated to pH 8.3 (T1). Next, 0.1 mL bromophenol blue was added, and the leachate titrated to pH 4.1 (T2) (the value reached to the titration endpoint of bromophenol blue). From T1 and T2, the concentration of carbonate (CO_3^{2-}) and bicarbonate (HCO_3^-) were determined respectively.

3. Results and discussion

XRD results (Fig. 1) indicated that the minerals were chemically bonded alkali (calcite ($CaCO_3$), cancrinite ($Na_6CaAlSi(CO_3)O_{24}\cdot 2H_2O$) and hydrogarnet ($Ca_3AlFe_2(SiO_4)(OH)_4$)), together with other minerals including hematite (Fe_2O_3), goethite (FeOOH), diaspore (AlO(OH)), gibbsite ($Al(OH)_3$) and perovskite ($CaTiO_3$)).

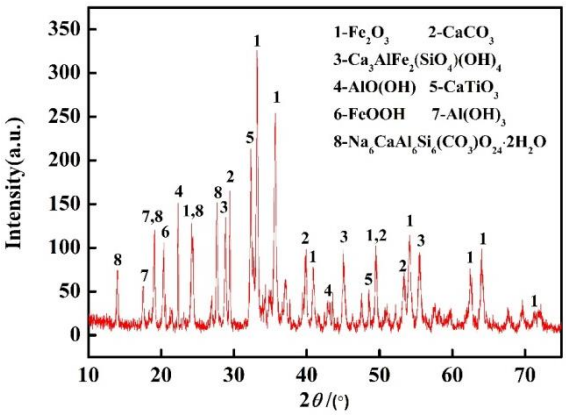

Fig. 1 XRD patterns collected from the raw BR.

Table 1 Soluble cations from the dissolution of soluble alkali.

Element	Na	Al	K	Ca	Mg
Concentration(mg/L)	1161	52.50	81.82	2.24	0.18

3.1 Effect of L/S ratio

Effect of L/S ratio on pH, alkaline anion content and leachate alkalinity are presented in Tables 2 and 3 (25 °C, 23 h, 1st stage leaching). The pH of the supernatant and the concentration of the main alkaline anions changed with increasing L/S ratio (Table 2). The pH decreased with increasing L/S ratio probably because of the dilution effect from the water. In contrast, alkaline anions reached a maximum concentration when the L/S ratio was 2 mL/g, and the concentration of CO_3^{2-} , HCO_3^-, $Al(OH)_4^-$ reached 37.20, 9.90 and 1.90 mmol/L respectively. This then slowly decreased with an increase in L/S ratio. Alkaline anion concentrations were in the following decreasing order: $c(CO_3^{2-}) > c(HCO_3^-) > c[Al(OH)_4^-] > c(OH^-)$. The L/S ratio of 2 mL/g may be used to regulate

alkalinity due to the high concentration of alkaline anions and is relevant to the rate of reaction.

Nevertheless, leaching of alkaline anions should be taken into consideration because the leaching concentration couldn't explain the effect of the different L/S ratio. It's clear that key points of L/S ratio were 2, 4 and 5 mL/g (Table 3). Alkaline anion concentration slowly changed after 2 mL/g, but when the L/S ratio reached 5 mL/g, the content was unchanged. These three points were selected for the experimental conditions, and the molarity of alkaline anions at 4 mL/g was 2.24 mmol. A L/S ratio of 4 mL/g can therefore be regarded as the condition following the single-factor experiment.

Table 2 Effect of L/S ratio on pH, alkaline anions and alkalinity of leachates.

Parameter	Units	L/S ratio						
		1	2	3	4	5	6	7
pH	Units	10.67±0.12	10.45±0.10	10.24±0.07	10.14±0.07	10.04±0.07	9.97±0.07	9.94±0.08
$c(CO_3^{2-})$	mmol/L	31.40±0.70	37.20±0.78	22.90±1.21	19.90±0.67	16.30±0.37	12.30±0.64	10.90±0.67
$c(HCO_3^-)$	mmol/L	6.40±0.33	9.90±0.36	8.30±0.14	6.70±0.22	6.40±0.16	6.30±0.22	5.50±0.29
$c[Al(OH)_4^-]$	mmol/L	1.00±0.07	1.90±0.03	1.50±0.03	1.30±0.02	1.10±0.04	1.00±0.02	0.90±0.03
$c(OH^-)$	mmol/L	0.47±0.06	0.29±0.04	0.17±0.04	0.14±0.03	0.11±0.02	0.09±0.02	0.09±0.02
Alkalinity*	mmol/L	39.27±1.03	49.29±0.50	32.87±1.13	28.04±0.50	23.91±0.22	19.69±0.85	17.39±0.73

*Alkalinity = $c(CO_3^{2-})+c(HCO_3^-)+c[Al(OH)_4^-]+c(OH^-)$

Table 3 Effect of liquid to solid on the leaching molarity of alkaline anions.

Parameter	Units	L/S ratio						
		1	2	3	4	5	6	7
$n(CO_3^{2-})$	mmol	0.63±0.01	1.49±0.03	1.37±0.07	1.59±0.05	1.63±0.04	1.48±0.08	1.53±0.09
$n(HCO_3^-)$	mmol	0.13±0.01	0.40±0.01	0.50±0.01	0.54±0.02	0.64±0.02	0.76±0.03	0.77±0.04
$n[Al(OH)_4^-]$	mmol	0.02±0.01	0.08±0.01	0.09±0.02	0.10±0.01	0.11±0.01	0.12±0.02	0.13±0.02
$n(OH^-)$	mmol	0.01	0.01	0.01	0.01	0.01	0.01	0.01
Total	mmol	0.79±0.02	1.98±0.02	1.97±0.03	2.24±0.03	2.39±0.02	2.37±0.04	2.44±0.05

3.2 Effect of leaching temperature

The dissolution behavior of alkaline anions with increasing leaching temperature are presented in Fig 2 (L/S ratio of 4 mL/g, 23 h, 1st stage leaching).

Carbonate concentration changed with increasing leaching temperature (Fig. 2), reaching 18.2 mmol/L at 25 °C, dissolving slightly with increasing temperature until dissolution equilibrium was reached. Concentrations of HCO_3^-, $Al(OH)_4^-$ and OH^- were lower than carbonates, and no change was observed with increasing temperature. This demonstrates that carbonate in the BR may continuously dissolve with increasing temperature until dissolution is reached. pH increased rapidly with increasing temperature (<30 °C) (Fig 3) but eventually decreased. Total concentrations of alkaline anions increased slowly (>20 °C) due to dissolution of carbonate, the change in pH and alkalinity denoting balance of reaction and dissolution. Alkalinity reached 27.11 mmol/L at 25 °C. The single-factor experiment should therefore be conducted at 25 and 20°C.

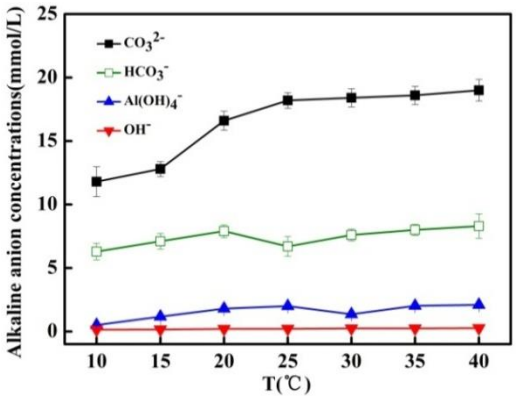

Fig. 2 Effect of temperature on changes in alkaline anion concentrations.

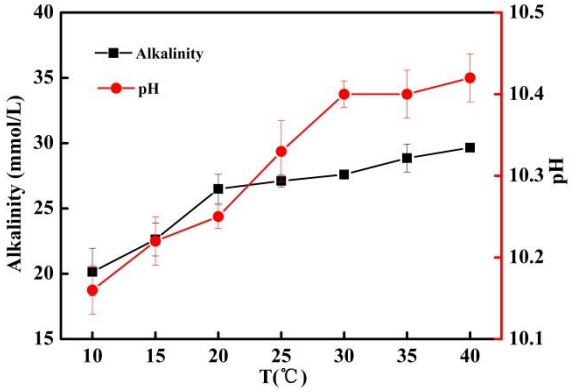

Fig. 3 Effect of leaching temperature on changes in pH and alkalinity.

3.3 Effect of leaching time

Dissolution behavior of alkaline anions with increasing leaching time are presented in Fig 4 under the L/S ratio of 4 mL/g, 25 °C, 1st stage leaching.

Leaching time appeared to affect carbonate concentration (Fig. 4), reaching 17.3 mmol/L at 13 h, but tapering off at this point. Concentrations of HCO_3^-, $Al(OH)_4^-$ and OH^- changed only slightly

with increasing leaching time, being almost completely leached within the first hour. Carbonate is a critical alkaline anion in BR, but alkaline anions originating from the dissolution of chemical bonded alkali or free alkali may also be involved. In leachates, pH increased but then remained at 10.30. Alkalinity reached 17.3 mmol/L at 13 h, with no change after this (Fig. 5). Leaching times of 13, 18 and 23 h may be considered as the orthogonal experimental conditions.

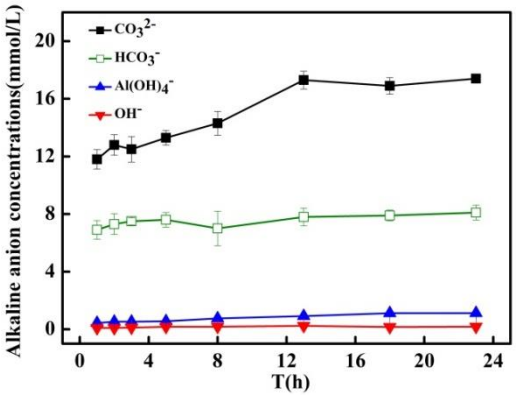

Fig. 4 Effect of leaching time on changes in alkaline anion concentrations.

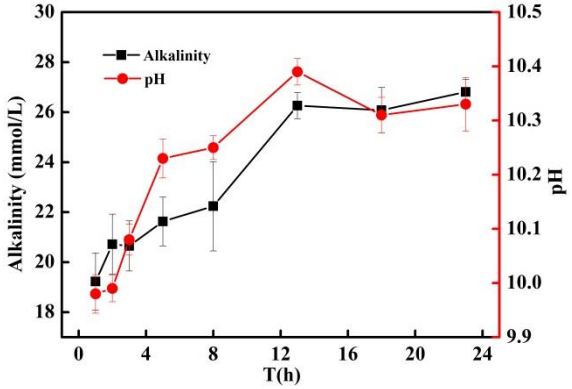

Fig. 5 Effect of leaching time on changes in pH and alkalinity.

3.4 Orthogonal experimental analysis for optimized leaching conditions

Orthogonal experiments were used to optimize leaching conditions of the alkaline anions; factors and levels are presented in Table 4, results are presented in Table 5. Table 5 reveals that the effect of leaching factors was as follows: temperature > liquid to solid ratio > time. This implies that temperature was the main factor influencing leaching rate. It is clear that the dissolution and diffusion of alkaline anions is closely related to temperature.

Table 4 Orthogonal experiment factors and levels.

Level	Factors			
	Residue mass, A/g	Ratio of liquid to solid, B/(mL/g)	Temperature, C/(°C)	Time, D/(h)
1	20	2	20	13
2	20	4	25	18
3	20	5	30	23

Table 5 Results of orthogonal experiments.

Level	Factor				
	Residue mass, A/g	Ratio of liquid to solid, B/(mL/g)	Temperature, C/(°C)	Time, D/(h)	Leaching mole* F/(mmol)
1	20	2	20	13	1.58
2	20	2	25	18	1.89
3	20	2	30	23	2.21
4	20	4	20	18	2.00
5	20	4	25	23	2.21
6	20	4	30	13	2.34
7	20	5	20	23	2.03
8	20	5	25	13	2.19
9	20	5	30	18	2.32
		1.673	1.703	1.820	
		1.940	1.857	1.857	
		1.953	2.007	1.890	
R		0.290	0.420	0.113	

*Leaching mole = $n(CO_3^{2-})+n(HCO_3^-)+n(Al(OH)_4^-+n(OH^-)$

3.5 Dissolution equilibrium of multiple leaching stage

Following optimized condition, the molarity of alkaline anions rapidly reduced with increasing leaching stage (Fig. 6 A) . Carbonate and bicarbonate reached 1.52 and 0.49 mmol in leachates at the first stage, respectively.. Alkaline anions showed almost no change after the third stage.

According to the dissolution equilibrium of alkali in the solid-liquid phase, alkaline anions from the dissolution of free alkali were completely leached by the sixth stage. The concentrations of alkaline anions generated from the dissolution equilibrium of the chemical bonded alkali are shown in Table 6. Dissolution of chemical bonded alkali were unaffected by the higher concentration of alkaline anions when soluble alkalinity was completely removed. Only a few alkaline anions (calcite, cancrinite, hydrogarnet) were leached at the sixth stage. Concentrations of carbonate, bicarbonate, aluminate and hydroxide were 3.1, 3.8, 0.21, 0.04 mmol/L respectively with pH reaching 9.57. Assuming the dissolution balance of chemical bonded alkali wouldn't be affected by leaching stage, the calculation equations (10), (11), (12) were defined and the content of alkaline anions originating from the dissolution of free alkali were calculated (Table 6). Alkaline anions from dissolution of free alkali improved the alkalinity of the liquid phase in BR.

The effect of leaching stage on the dissolution of free alkali is shown in Fig. 6 B. During the first stage, carbonate and bicarbonate molarity reached 1.4 mmol and 0.34 mmol in leachates, respectively. Alkaline anions were almost unchanged after the third stage. Alkalinity reached 69.78 mmol/L (Table 6), and the leaching rate was calculated using equation (13) (Fig 7). Leaching rate reached 67 % during the first stage, reducing to 19 %, 9 %, 4 %, 2 % and 0 %, at the second to sixth stages, respectively. The total leaching rate was 86 % within two leaching stages. Table 6 reveals that the critical alkaline anion from dissolution of free alkali was CO_3^{2-} and its concentration reached 52.1 mmol/L, followed by HCO_3^-, 13.6 mmol/L.

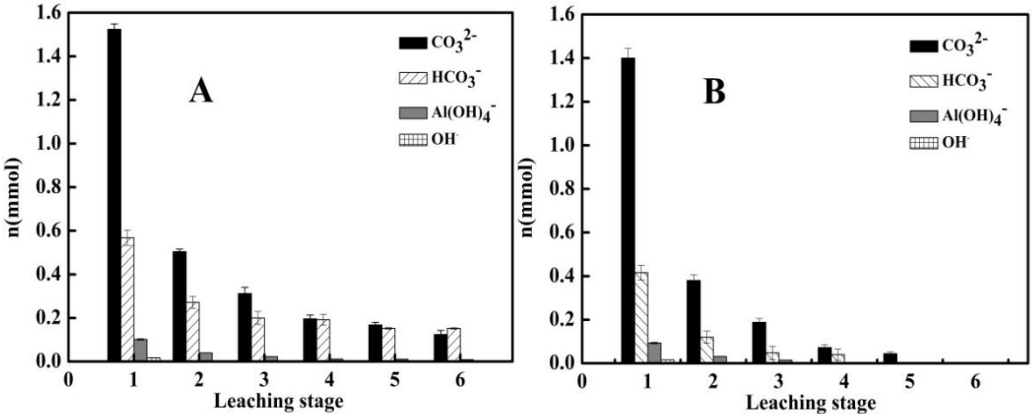

Fig. 6 Effect of leaching stage on the content of alkaline anion (A) and free alkaline anions (B).

$$Fa_n = Ls_n - C_b \quad (10)$$

$$C_b = Ls_6 \quad (11)$$

$$Fa = \sum_{n=1}^{5} Fa_n = \sum_{n=1}^{5} Ls_n - 5Ls_6 = \sum_{n=1}^{5} Ls_n - 5C_b \quad (12)$$

$$R_n = \frac{Fa_n}{Fa} \times 100\% \quad (13)$$

n - Leaching stage (which can be 1, 2, 3, 4, 5, 6)

Fa - Total concentration of alkaline anions from the dissolution of free alkali, mmol/L

C_b - Concentration of alkaline anions from the dissolution of chemical bonded alkali, mmol/L

Ls - Concentration of alkaline anions from the different leaching stages, mmol/L

R_n - Leaching rate, %

Table 6 Leaching characteristics of chemical bonded alkali and free alkali in BR.

Parameter	Units	Chemical bonded alkali [a]	Free alkali [b]	Free alkali [c]
pH	Units	9.57	10.47	> 10.47
$c(CO_3^{2-})$	mmol/L	3.10	35.00	52.10
$c(HCO_3^-)$	mmol/L	3.80	10.40	13.6
$c[Al(OH)_4^-]$	mmol/L	0.21	1.73	3.62
$c(OH^-)$	mmol/L	0.04	0.26	0.46
Alkalinity	mmol/L	7.15	47.39	69.78

[a] Data of chemical bonded alkali calculated from the sixth leaching stage.

[b] Data of free alkali through 1st leaching stage were calculated by equations (10), (11).

[c] Data of free alkali through six leaching stage were calculated by equations (10), (11) and (12).

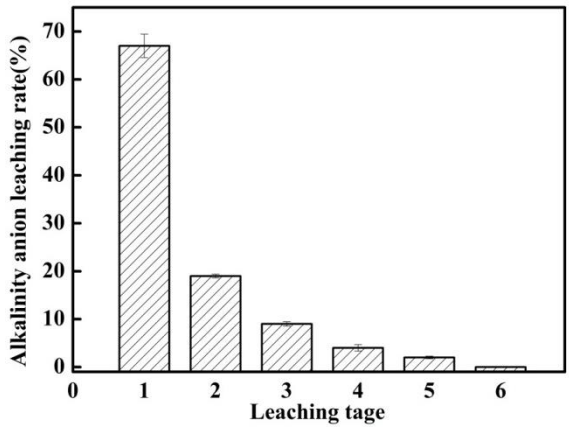

Fig. 7 Effect of leaching stage on leaching rate from the dissolution of free alkali.

3.6 Leaching kinetics of critical anions

Due to the high soluble alkalinity in BR, the Stumm model may be applied to the leaching kinetics of the critical anions. The Shrinking Core Model (SCM) was used to evaluate the dissolution process of the solid phase whilst analyzing the leaching process of sodium [6, 33]. The critical anion CO_3^{2-} was the main source of high alkalinity in the liquid phase of BR. It is therefore necessary to analyze its leaching process. The following two expressions of leaching kinetics can be used.

The Stumm Model [34]

$$\ln\frac{C_x}{C_x - C_t} = K_q t + Z \quad (14)$$

t - Reaction time, s

Z - Constant

C_x - Concentrations of carbonate in dissolution equilibrium, mmol/L

C_t- Concentrations of carbonate at the time of t, mmol/L

K_q- Kinetics rate constant

SCM diffusion model

$$K_a t = 1 - 2\frac{\alpha}{3} - (1-\alpha)^{2/3} \quad (15)$$

α - leaching rate (%)

K_a -Rate constant of internal diffusion

Leaching data at different temperatures produced a good fit using the Stumm Model (Fig. 8 and Fig. 9), illustrating that leaching of CO_3^2 from the dissolution of free alkali was controlled by solid film diffusion. Its rate increased with increasing L/S ratio and temperature, whilst the diffusion rate of water into interior particles was also another factor. Based on the diffusion constants at different temperatures, the plots of $\ln(K_q)$ versus temperature were established by the Arrhenius equation. The result (Fig. 10) observed with the correlation coefficient (R^2) was above 0.99 at the different temperatures. The apparent activation energy (Ea) was 10.24 KJ/mol, further illustrating that the diffusion rate of CO_3^{2-} was controlled by solid film diffusion.

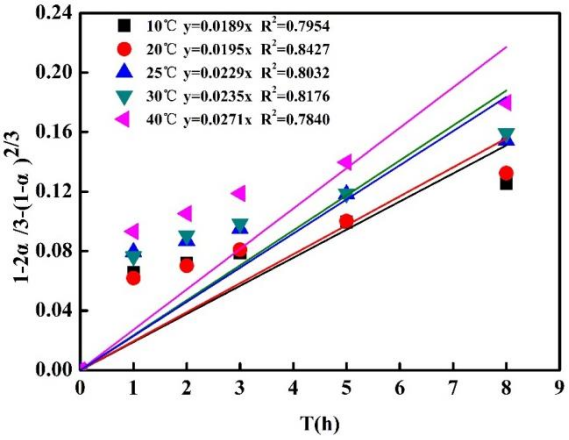

Fig. 8 Plots of [1-2α/3-(1-α)$^{2/3}$] versus time at different temperatures.

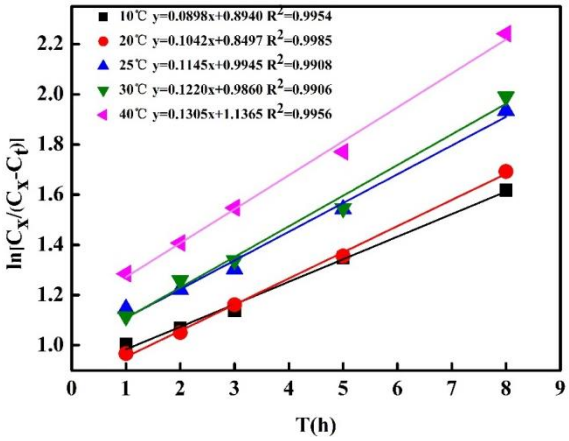

Fig. 9 Plots of In[Cx/(Cx-Ct)] versus time at different temperatures.

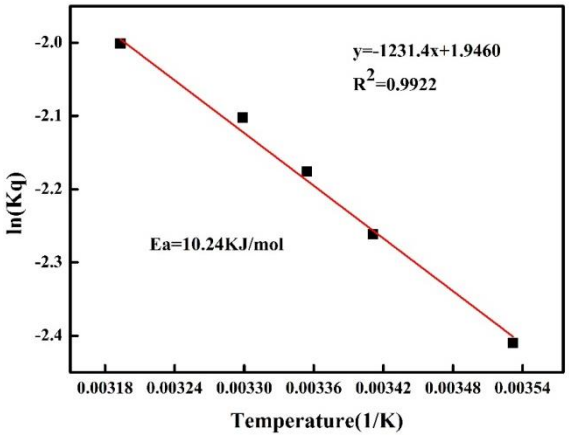

Fig. 10 Plots of ln(Kq) versus temperature of water leaching.

4. Conclusions

1) Leaching of soluble alkaline anions (CO_3^{2-}, HCO_3^-, $Al(OH)_4^-$, OH^-) reached 86 % with a L/S ratio of 2 mL/g, at 30 °C, over 23 h during a two stage water leaching investigation, whilst pH reached 9.78.

2) Approximately 88 % of alkaline anions were leached from the dissolution of free alkali during the first stage with the remainder originating from alkaline minerals (calcite, cancrinite and hydrogarnet).

3) The alkaline anion CO_3^{2-} accounted for 75 % of the total soluble alkalinity (52.1 mmol/L), with HCO_3^- accounting for 19 %.

4) Carbonate leaching was controlled by solid film diffusion using the Stumm Model, with an activation energy of 10.24 KJ/mol.

References

[1] LI Xiao-bin, LIU Nan, QI Tian-gui, WANG Yi-lin, ZHOU Qiu-sheng, PENG Zhi-hong, LIU Gui-hua. Conversion of ferric oxide to magnetite by hydrothermal reduction in Bayer digestion process [J]. Transactions of Nonferrous Metals Society of China, 2015, 25: 3467-3474.

[2] KONG Xiang-feng, JIANG Xing-xing, XUE Sheng-guo, HUANG Ling, HARTLEY W, WU Chuan, LI Xiao-fei. Migration and distribution of salinity in bauxite residue during water leaching [J]. Transactions of Nonferrous Metals Society of China, 2017. (in Press)

[3] XUE Sheng-guo, KONG Xiang-feng, ZHU Feng, HARTLEY W, LI Xiao-fei, LI Yi-wei. Proposal for management and alkalinity transformation of bauxite residue in China [J]. Environmental Science and Pollution Research, 2016, 13:12822-12834.

[4] KIRWAN L J, HARTSHORN A, MCMONAGLE J B, FLEMING L, FUNNELL D. Chemistry of bauxite residue neutralization and aspects to implementation [J]. International Journal of Mineral Processing, 2013, 119: 40-50.

[5] XUE Sheng-guo, ZHU Feng, KONG Xiang-feng, WU Chuan, HUANG Ling, HUANG Nan, HARTLEY W. A review of the characterization and revegetation of bauxite residues (Red mud) [J]. Environmental Science and Pollution Research, 2016, 23:1120-1132.

[6] ZHU Xiao-bo, LI Wang, GUAN Xue-mao. An active dealkalization of red mud with roasting and water leaching [J]. Journal of Hazardous Materials, 2015, 286: 85-91.

[7] ZHU Feng, HUANG Nan, XUE Sheng-guo, HARTLEY W, HAN Fu-song, LI Yi-wei. Effects of binding materials on micro-aggregate size distribution in bauxite residues [J]. Environmental Science and Pollution Research, 23: 23867-23875.

[8] XUE Sheng-guo, SHI Li-zheng, WU Chuan, WU Hui, QIN Yan-yan, PAN Wei-song, HARTLEY W, CUI Meng-qian. Cadmium, lead, and arsenic contamination in paddy soils of a mining area and their exposure effects on human HEPG2 and keratinocyte cell-lines [J]. Environmental Research, 2017, 156: 23-30

[9] LU Qing-Hua, HU Yue-Hua. Synthesis of aluminum tri-polyphosphate anticorrosion pigment from bauxite tailings [J]. Transactions of Nonferrous Metals Society of China, 2012, 22: 483-488.

[10] WU Chuan, HUANG Liu, XUE Sheng-guo, PAN Wei-song, ZOU Qi, HARTLEY W, WONG Ming-hung. Oxic and anoxic conditions affect arsenic (As) accumulation and arsenite transporter expression in rice [J]. Chemosphere, 2017, 168: 969-975.

[11] ZHU Feng, LI Yu-bing, XUE Sheng-guo, HARTLEY W, WU Hao. Effects of iron-aluminium

oxides and organic carbon on aggregate stability of bauxite residues [J]. Environmental Science and Pollution Research, 2016, 23: 9073-9081.

[12] MAYES W M, JARVIS A P, BURKE I T, WALTON M, FEIGL V, KLEBERCZ O, GRUIZ K. Dispersal and attenuation of trace contaminants downstream of the Ajka bauxite residue (red mud) depository failure Hungary [J]. Environmental Science & Technology, 2011, 45: 5147-5155.

[13] ZHU Feng, LI Xiao-fei, XUE Sheng-guo, HARTLEY W, WU Chuan, HAN Fu-song. Natural plant colonization improves the physical condition of bauxite residue over time [J]. Environmental Science and Pollution Research, 2016 23: 22897-22905.

[14] LIU Wan-chao, CHEN Xiang-qing Q, LI Wang-xing, YU Yan-fen, YAN Kun. Environmental assessment, management and utilization of red mud in China [J]. Journal of Cleaner Production, 2014, 84: 606-610.

[15] ZHU Feng, ZHOU Jia-yi, XUE Sheng-guo, HARTLEY W, WU Chuan, GUO Ying. Aging of bauxite residue in association of regeneration: a comparison of methods to determine aggregate stability & erosion resistance [J]. Ecological Engineering, 2016, 92: 47-54.

[16] GOLOTAN J B, CHEN Cheng-rong, PHILLIPS I R, ELSER J J. Shifts in leaf N:Pstoichiometry during rehabilitation in highly alkaline bauxite processing residue sand [J]. Scientific Reports, 2015, 5: 1-12.

[17] ZHU Feng, XUE Sheng-guo, HARTLEY W, HUANG Ling, WU Chuan, LI Xiao-fei. Novel predictors of soil genesis following natural weathering process of bauxite residue [J]. Environmental Science and Pollution Research, 2016, 23: 1-8.

[18] COURTNEY R, KIRWAN L. Gypsum amendment of alkaline bauxite residue - Plant available aluminium and implications for grassland restoration [J]. Ecological Engineering, 2012, 42: 279-282.

[19] ZHU Feng, HOU Jing-tao, XUE Sheng-guo, WU Chuan, WANG Qiong-li, HARTLEY W. Vermicompost and Gypsum amendments improve aggregate formation in bauxite residue [J]. Land Degradation and Development, 2017, DOI: 10.1002/ldr.2737.

[20] MENZIES N W, FULTON I M, MORRELL W J. Seawater Neutralization of Alkaline Bauxite [J]. Journal of Environmental Quality, 2004, 33: 1877-84.

[21] HAN Y S, JI S, LEE P K, OH C. Bauxite residue neutralization with simultaneous mineral carbonation using atmospheric CO_2[J]. Journal of Hazardous Materials, 2017, 326: 87-93.

[22] ZHU Feng, LIAO Jia-xing, XUE Sheng-guo, HARTLEY W, ZOU Qi, WU Hao. Evaluation of aggregate microstructures following natural regeneration in bauxite residue as characterized by synchrotron-based X-ray micro-computed tomography [J]. Science of Total Environmental, 2016, 573: 155-163.

[23] KONG Xiang-feng, LI Meng, XUE Sheng-guo, HARTLEY W, CHEN Cheng-rong, WU Chuan, LI Xiao-fei, LI Yi-wei. Acid transformation of bauxite residue: Conversion of its alkaline characteristics [J]. Journal of Hazardous Materials, 2017, 324: 382-390.

[24] JONES B E H, HAYNES R J. Bauxite processing residue: A critical review of its formation, properties, storage, and revegetation [J]. Critical Reviews Environmental Science and Technology, 2011, 41: 271-315.

[25] BORGES A J P, HAUSER-DAVIS R A, OLIVEIRA T F D. Cleaner red mud residue production at an alumina plant by applying experimental design techniques in the filtration stage [J]. Journal of Cleaner Production, 2011, 19: 1763-1769.

[26] HUANG Yan-fang, CHAI Wen-cui, HAN Gui-hong, WANG Wen-juan, YANG Shu-zhen, LIU Jiong-tian. A perspective of stepwise utilisation of Bayer red mud: Step two-Extracting and recovering Ti from Ti-enriched tailing with acid leaching and precipitate flotation [J]. Journal of Hazardous Materials, 2016, 307: 318-327.

[27] YANG Yang, WANG Xue-wen, WANG Ming-yu, WANG Hua-guang, XIAN Peng-fei. Recovery of iron from red mud by selective leach with oxalic acid [J]. Hydrometallurgy, 2015, 157: 239-245.

[28] KONG Xiang-feng, GUO Ying, XUE Sheng-guo, HARTLEY W, WU Chuan, YE Yu-zhen, CHENG Qing-yu. Natural evolution of alkaline characteristics in bauxite residue [J]. Journal of Cleaner Production, 2017, 143: 224-230.

[29] SANTINI T C, HINZ C, RATE A W, CARTER C M, GILKES R J. In situ neutralisation of uncarbonated bauxite residue mud by cross layer leaching with carbonated bauxite residue mud [J]. Journal of Hazardous Materials, 2011, 194: 119-127.

[30] RADOMIROVIC T, SMITH P, SOUTHAM D, TASHI S, JONES F. Crystallization of sodalite particles under Bayer-type conditions [J]. Hydrometallurgy, 2013, 137: 84-91.

[31] PARADIS M, DUCHESNE J, LAMONTAGNE A, ISABEL D. Long-term neutralisation potential of red mud bauxite with brine amendment for the neutralisation of acidic mine tailings [J]. Applied Geochemistry, 2007, 22: 2326-2333.

[32] KINNARINEN T, HOLLIDAY L, HAKKINEN A. Dissolution of sodium, aluminum and caustic compounds from bauxite residues [J]. Minerals Engineering, 2015, 79: 143-151.

[33] FERRIER R J, CAI L P, LIN Q Y, GORMAN G J, NEETHLING S J. Models for apparent reaction kinetics in heap leaching: A new semi-empirical approach and its comparison to shrinking core and other particle-scale models [J]. Hydrometallurgy, 2016, 166: 22–33.

[34] STUMM W, MORGAN J J. Introduction of natural water body chemical balance [M]. Translated by TANG Hong-xiao. Beijing: Science Press, 1987: 129–134. (in Chinese)

赤泥碱性阴离子浸出优化及溶解行为

李晓飞[1]，叶羽真[1]，薛生国[1,2]，吴川[1,2]，孔祥峰[1]，William Hartley[3]，李义伟[1]
1. 中南大学 冶金与环境学院，长沙 410083；
2. 中南大学 国家重金属污染防治工程术研究中心，长沙 410083；
3. Harper Adams University Crop and Environment Sciences Department, Newport, Shropshire, United Kingdom TF10 8NB

摘 要：赤泥是氧化铝工业生产过程中产生的高碱性固体废弃物。基于单因素-正交实验开展赤泥碱性阴离子浸出特性研究，探讨最佳浸出条件和溶解过程。结果表明：在液固比2、浸出温度30℃、浸出时间23 h、2次浸出条件下，可溶性碱性阴离子(CO_3^{2-}, HCO_3^-, $Al(OH)_4^-$, OH^-)的最佳浸出率达86 %；赤泥1次浸出液中，88 %的阴离子来源于可溶性碱（NaOH、碳酸盐、碳酸氢盐、$NaAl(OH)_4$），12 %的阴离子来源于化学结合碱（方解石、钙霞石、水化石榴石）；最佳浸出条件下，可溶性碱性离子浸出总浓度为69.78 mmol/ L，CO_3^{2-}约占75 %；碳酸盐溶解反应的表观活化能 E_a=10.24 KJ/mol，主要受固膜扩散控制。

关键词：赤泥； 碱性阴离子； CO_3^{2-}； 浸出优化； 溶解行为